Applied Catalysis B: Environmental 88 (2009) 127–134

Contents lists available at ScienceDirect

Applied Catalysis B: Environmental

journal homepage: www.elsevier.com/locate/apcatb

Synthesis of Fe,Al-pillared clays starting from the Al,Fe-polymeric precursor: Effect of synthesis parameters on textural and catalytic properties

M.N. Timofeeva [a,*], S.Ts. Khankhasaeva [b], Yu.A. Chesalov [a,c], S.V. Tsybulya [a,c], V.N. Panchenko [a], E.Ts. Dashinamzhilova [b]

[a] Boreskov Institute of Catalysis SB RAS, Prospekt Akad. Lavrentieva 5, 630090, Novosibirsk, Russian Federation
[b] Baikal Institute of Nature Management SB RAS, Ulan-Ude, Str. Sakh'yanova 8, 670047, Ulan-Ude, Russian Federation
[c] Novosibirsk State University, Prospekt Akad. Koptyuga 2, Novosibirsk 630090, Russian Federation

ARTICLE INFO

Article history:
Received 19 May 2008
Received in revised form 18 September 2008
Accepted 19 September 2008
Available online 27 September 2008

Keywords:
Iron-containing pillared clay
Effect of synthesis parameters
Hydrogen peroxide
Phenol
Dye
Oxidation

ABSTRACT

Effect of OH/(Fe + Al) ratio, aging time of Fe,Al-containing pillaring solution on physicochemical properties of Fe,Al-pillared clays (Fe,Al-PILCs) obtained from Mukhortala (Buryatia) montmorillonites and the change of these properties with the calcination temperature were examined. Characterization studies were performed by use of XRD, FTIR, DR-UV-vis, ^{27}Al NMR and N_2-adsorption/desorption analysis. It was found that the prolonged aging time of the Fe,Al-solution (Al/Fe = 10/1) favours the increase in total surface area, total pore-volume and micropore volume of Fe,Al-PILCs. The relationships between preparation conditions, iron state, catalytic activity and stability to leaching were revealed in hydrogen peroxide oxidation of phenol and monoazo dye acid chrome dark-blue (ACDB). The state of iron atoms can be controlled by Al/Fe and OH/(Fe + Al) ratios, aging period of Fe,Al-pillaring solution and calcination temperature. The increase in Al/Fe ratio and calcination temperature from 400 °C to 500 °C reduces to the decrease in the formation of oligomeric iron species. The increase in aging time of Fe,Al-pillaring solution reduced to decrease in iron leaching and increase in reaction rate due to the formation of isolated iron species.

1. Introduction

Phenol and phenol derivatives have been warranted more attention in the field of industrial wasterwaters in the past tree decades. It is well-known that elimination of phenol is mostly based on peroxide oxidation to produce CO_2 and H_2O in the presence of homogeneous and/or heterogeneous catalytic systems of the Fenton type (H_2O_2–Fe^{2+}) [1–3]. Various heterogeneous Fe-containing systems have been evaluated as catalysts for PhOH oxidation with H_2O_2. However many of these systems possess a certain disadvantages. Main of these disadvantages is low activity and stability. Activity of overwhelming majority systems in phenol peroxide oxidation is maximal at pH 3–4 and is accompanied with substantial iron leaching [4–7]. Layered silicate clays intercalated by polymeric inorganic oxocations are perspective catalysts due to high stability, microporosity, larger surface area and existence of acid sites (Brönsted and Lewis sites) [5–9]. Catalysts based on pillared interlayered clays (PILCs) have been actively investigated in the last years. Most of these have focused on application of Al,Fe-mixed systems for phenol peroxide oxidation due to their high activity at pH 5–6 [7,10]. Various pillaring agents and various pillaring processes have been investigated in an effort to improve the porous and catalytic properties of these systems. Most of the research on PILCs has been focused on Al_xFe_y polyoxocation as a pillaring precursor. However, until now it is not absolutely clear correlation between degree of hydrolysis of the Fe,Al-pillaring solution, the calcination temperature and main properties of PILCs, such as textural, structural and catalytic properties. Thus, the nature of pillaring agent strongly depends on the OH/metal ratio. According to literature data [11,12] the degree of hydrolysis of a pillaring solution ($0.5 < OH/Al < 2.5$) affects the micropore volume and the overall surface area of Al-PILCs. A value of 2.2 was the optimum. It is worth noting that maximum interlayer distance can be obtained when the Al_{13}^{7+} cation is present in a pillaring solution [12]. The total surface area, micropore area and pore volume also increased with aging time of the Al_{13}-solution [8,13] due to the transformation of Al_{13}^{7+} into $Al_{24}O_{72}$ (Al_{13} dimer) and other

* Corresponding author. Tel.: +7 383 330 72 84; fax: +7 383 330 50 86.
E-mail addresses: timofeeva@catalysis.ru (M.N. Timofeeva), shan@binm.bscnet.ru (S.Ts. Khankhasaeva).

0926-3373/$ – see front matter © 2008 Elsevier B.V. All rights reserved.
doi:10.1016/j.apcatb.2008.09.013

Table 1
Textural data of Fe,Al-PILCs.

	Sample[a]	Conditions of synthesis		A_{BET} ($m^2\,g^{-1}$)	S_μ ($m^2\,g^{-1}$)	ΣV_{pore} ($cm^3\,g^{-1}$)	V_μ ($cm^3\,g^{-1}$)	D_{pore} (Å)	$d_{0\,0\,1}$
		Time (days[b])	OH/(Fe + Al)						
1	Na-clay	–	–	141	n.d.	0.20	n.d.	57	15.4
2	Fe,Al-PILC(I)-1	1	2.4	132	30	0.19	0.016	58	17.2
3	Fe,Al-PILC(I)-7	7		219	101	0.23	0.048	42	17.8
4	Fe,Al-PILC(I)-12	12		209	96	0.24	0.046	46	17.8
5	Fe,Al-PILC(I)-21	21		215	106	0.22	0.051	41	17.8
6	Fe,Al-PILC(II)-1	1	2.0	125	29	0.18	0.014	58	17.2
7	Fe,Al-PILC(II)-21	21		236	113	0.25	0.054	42	17.8

[a] Samples calcinated at 500 °C for 2 h.
[b] Aging time of pillaring solution.

polynuclear cations [14]. The formation of mixed polyoxocation $[Fe_xAl_{13-x}O_4(OH)_{24}(H_2O)_{12}]^{7+}$ (Fe_xAl_{12-x}) also depends on OH/(Al + Fe) and Al/Fe ratios [15–18]. The higher Al/Fe and OH/(Al + Fe) ratios, the more amount of polyoxocation forms in solution. In our previous work [7], we investigated the influence of different methods of preparation of Fe,Al-PILCs on the catalytic activity in wet phenol peroxide oxidation. We determined that catalytic system (Fe,Al-PILC, method I) synthesized from naturally occurring montmorillonites by substitution of interlayer ions by Fe_xAl_{12-x} cation (Al/Fe = 10/1 and OH/(Al + Fe) = 2.0) was more stable to leaching of iron species and more active than system prepared by adsorption of iron ions onto Al-PILC (method II). According to SEM data the main reason of this difference was the formation of iron oxide phase in sample prepared by method II.

In this work the effect of OH/(Fe + Al) ratio, aging time of Fe,Al-containing pillaring solution on physicochemical properties of Fe,Al-pillared clays (Fe,Al-PILCs) prepared by method I and the change of these properties with the calcination temperature were examined. The catalytic properties of Fe,Al-PILCs were assessed in peroxide oxidation of phenol and monoazo dye acid chrome dark-blue (ACDB). The relationships between preparation conditions, iron state, catalytic activity and stability to leaching were revealed.

2. Experimental

2.1. Materials

The natural layered aluminosilicate was obtained from a bed located in Mukhortala, Buryatia. The mineral contains more than 95% of a calcium-rich montmorillonite with the total chemical composition: SiO_2: 65.5 wt.%; Al_2O_3: 14.3 wt.%; Fe_2O_3 and FeO: 1.1 wt.%; MgO: 1.4 wt.%; CaO: 1.1 wt.%; K_2O and Na_2O: 0.3 wt.%; MnO and TiO_2: 0.2 wt.%; H_2O: 16.1 wt.%. The sodium-containing layered aluminosilicate (Na-clay) used for the preparation of the pillared samples was synthesized by the treatment of the natural layered aluminosilicate with 1 M NaCl at a ratio 1–100 (w/w) between solid and liquid phases at 80 °C for 2 h. This clay was ground and sieved to obtain a fraction of 20–40 μm.

2.2. Synthesis of pillared clay

Synthesis of Fe,Al-PILCs was performed using a procedure described in [7]. Na-clay was stirred (1 wt.% solution) in distilled water for about 24 h at 20 °C and then it was dispersed by ultrasonic dismemberment. The Al,Fe-pillaring solutions (Al/Fe = (10 − 6.5)/(1 − 6.5)) were prepared from mixing 0.2 M $AlCl_3$ and 0.1 M $FeCl_3$ with following hydrolysis using NaOH solution (OH/(Al + Fe) = 2.0 and 2.4). Solution of Al/Fe was added (0.6 ml/min) to the clay at room temperature and the mixture was storage for 1–21 days at room temperature. The intercalated clay was filtered by suction, washed with distilled water, dried in air and calcinated at 500 °C or 400 °C for 2 h. The designation of the samples and the main conditions of this synthesis are given in Table 1.

2.3. Instrumental measurements

The porous structure of supports was determined from the adsorption-desorption isotherm of N_2 (77 K) on a SORBI-M equipment. The specific surface area (S_{BET}) was calculated by the Brunauer–Emmett–Teller (BET) method. The X-ray diffraction patterns were measured on a X-ray diffractometer XTRA (Thermo-ARL) with Cu Kα (λ = 1.5418 Å) radiation.

The DR-UV-vis spectra were recorded on a UV-2501 PC Shimadzu spectrometer with a IRS-250A accessory in the 190–900 nm range with a resolution of 2 nm. $BaSO_4$ was used as standard. The samples in a form of powders were placed into a special cell for DR-UV-vis measurement. ^{27}Al NMR spectra were measured at room temperature on a MSL-400 Bruker NMR spectrometer at a frequency of 162 MHz, with a 50 kHz sweep width, 10 μs pulse width, and 0.2 s interpulse delay. The chemical shift was calibrated at 0 ppm with a solution of $AlCl_3$, using as internal standard. Infrared spectra were recorded on a BOMEM-MB-102 spectrometer in 4000–250 cm^{-1} range with a resolution of 4 cm^{-1} (compressed pellets of 2 mg of catalysts and 500 mg KBr). For IR transmission measurements, the Fe,Al-PILC(I)-21 grinded in an agate mortar were pressed into self-supporting wafers (density of the wafers obtained was 7–20 mg/cm^2) and pre-treated within the IR cell by heating at 300 °C in flowing air for 2 h before adsorption experiments. FTIR spectra were recorded on a Shimadzu FTIR-8300 in the 400–4000 cm^{-1} range with a resolution of 4 cm^{-1}, accumulating 50 scans. The IR cell was sealed with CaF_2 windows. CO adsorption was carried out at 80 K and equilibrium pressures of P_{CO} 0.5–76 Torr.

2.4. Catalytic tests

The phenol oxidation was carried out at 50 °C in a glass thermostated vessel equipped with a stirrer and a reflux condenser. The reactor was charged with a mixture of $PhOH/H_2O_2$ (30 wt.% in water) = 1:14 mol mol^{-1} (20 ml of 1×10^{-3} M phenol solution in water) and a catalyst (typically, 1.0 g L^{-1}). The phenol concentration in the solution was determined using UV–vis (Specord UV–vis M-40 instrument, λ = 273 nm, accuracy ±10%). The TOC concentration was determined by the Shimadzu TOC analyzer.

2.4.1. Recycling tests

After each cycle, the catalyst was separated, washed by H_2O, dried at 423 K in air during 4 h and then reused.

The monoazo dye acid chrome dark-blue ($C_{16}H_9O_9Na_2ClS_2N_2$, ACDB) oxidation was carried out at 25–75 °C in a glass thermostated vessel equipped with a stirrer and a reflux condenser. The reactor was charged with a mixture of $ACDB/H_2O_2$ (30 wt.% in

water) = 1/(38.4 – 120) mol mol^{-1} (20 ml of 1×10^{-4} M ACDB solution in water) and a catalyst (0.5–2.0 g L^{-1}). The ACDB concentration in the solution was determined using UV–vis (Agilent 8453 UV–vis instrument, λ = 540 nm, accuracy ±10%).

The iron content in PILC samples was determined by means of the following procedure. The iron was transformed into solution in the form of Fe^{3+} iron by boiling PILC in HNO_3–HCl mixture and then it was allowed to react with 1,10-phenanthroline. The absorbance of the iron–phenanthroline complex was measured by UV–vis at λ = 510 nm.

PhOH adsorption onto Fe,Al-PILCs was studied in a glass thermostated reactor under stirring at 50 °C. The reactor was loaded with 25 mg Fe,Al-PILC and 5 ml of a PhOH aqueous solution (1×10^{-3} M). At regular time intervals, aliquots were taken and the phenol concentration was determined by UV–vis at λ = 273 nm.

The titrant (0.2 M NaOH) was added in 0.1 ml portions to a 20 ml volume of Al- and/or Fe,Al-solution at 25 °C. The titrations were performed using the pH glass electrode, with an Ag/AgCl internal reference electrode and a KCl bridge. The pH meter was calibrated using standard pH buffers before the titration.

3. Results

3.1. Physicochemical studies of pillaring reagents

Effect of Al/Fe and OH/(Al + Fe) ratios on the composition of pillaring solution was studied by various physicochemical methods. Fig. 1 shows the evolution of the experimental potentiometric titration curves of $AlCl_3$ solution with aqueous NaOH as functional of the OH/Al ratio (R_M). As one can judge from Fig. 1, three regions are observed in titration curve of Al-solution. The region I (R_M 0/0.5) is usually assigned to the neutralization of free acid, that produced by spontaneous hydrolysis of $AlCl_3$ by NaOH. In region II the pH of mixture increases slowly, because added NaOH is consumed due to the formation of dimeric, trimeric and polynuclear hydrolysis products of $AlCl_3$ [19–21]. The pH of mixture sharply increases in region III. According to Refs. [22–25] polynuclear hydrolysis products of $AlCl_3$ can form in R_M region of 1.8 ÷ 2.5. Al_{13} species is a dominant Al species in freshly prepared solution and its content can reaches about 80% from total content of Al polynuclear species at R_M 2.3–2.4 [25]. At the same time the titration curve of mixed solution of $AlCl_3$ and $FeCl_3$ consists of four regions (Fig. 1, curve 2).

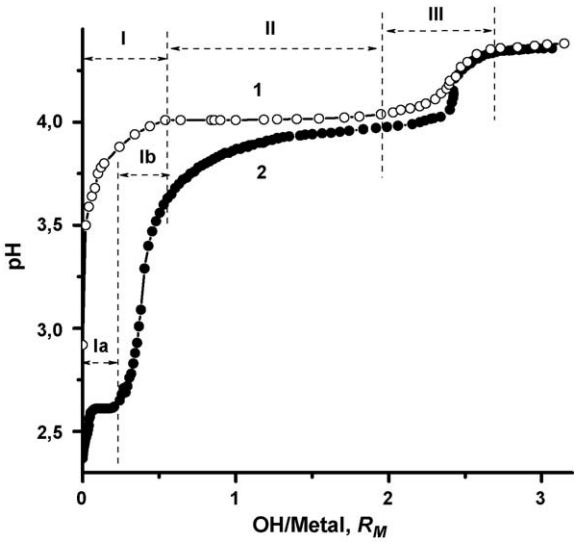

Fig. 1. Titration curve of 0.1 M $AlCl_3$ solution (1) and Fe,Al-solution ($AlCl_3$ 0.1 M, Al/Fe = 10/1) (2) at 25 °C.

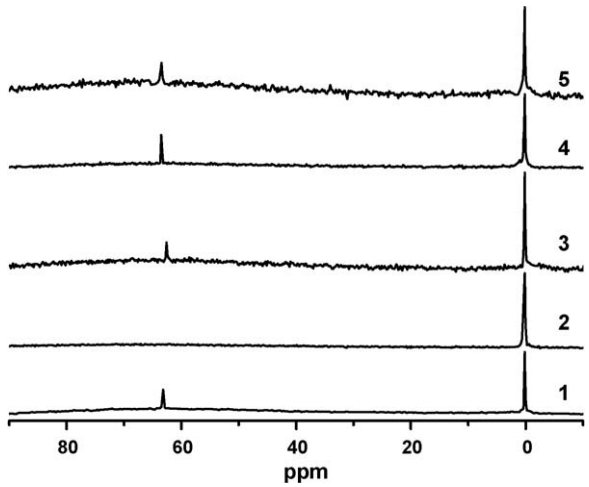

Fig. 2. ^{27}Al NMR spectra of Fe,Al-solutions: OH/(Fe + Al) = 2.0 and Al/Fe = 10/1, (1); OH/(Fe + Al) = 2.4 and Al/Fe = 7/6, (2), OH/(Fe + Al) = 2.4 and Al/Fe = 10/3, (3), OH/(Fe + Al) = 2.4 and Al/Fe = 10/1, (4) and (5). Spectra (1)–(4) were registered in a 7 days after preparing solution; spectrum (5) was registered in a 1 day.

Two parts can be discerned in region I. The region Ia is very likely caused by acid neutralization that produced by hydrolysis of $FeCl_3$, giving a $Fe(OH)^{2+}$, $Fe(OH)_2^{+}$ and/or $Fe_2(OH)_4^{2+}$ ions [21,26]. The increase in OH/(Al + Fe) ratio leads to the formation of mixed dimeric, trimeric and polynuclear hydrolysis products of $FeCl_3$ and $AlCl_3$. Probably, in R_M region of 2.0–2.4 mixed $FeAl_{12}$-complex forms due to the incorporation of Fe^{3+} ions into structure of Al_{13}^{7+} cation [15,27].

This is in agreement with ^{27}Al NMR spectroscopic data. The ^{27}NMR spectra of mixed Al,Fe-solution (Al/Fe = 10/1) with OH/(Al + Fe) = 2.0 and 2.4 are shown in Fig. 2 (spectra 1 and 4). Two signals were observed in spectra. The first signal at 0 ppm is assigned to monomeric Al species [28,29]. The second signal at 62.5 ppm attributed to Al atoms in fourfold coordination within a polymeric structure Al_{13}^{7+} complex [23,28,30,31]. It is interesting to note that the increase Al/Fe ratio leads to collapse of Al_{13}^{7+} complex (Fig. 2, spectra 2–4) due to the separate coagulation of Fe^{3+} and Al^{3+} ions.

The nature and coordination of iron ions in mixed base-hydrolyzed solutions of Al^{3+} and Fe^{3+} salts were characterized by UV–vis spectroscopy. Fig. 3 shows UV–vis spectra of Al, Fe-solutions with different OH/(Al + Fe) ratio. Bands at 220, 257 and 324 nm are observed in spectra of solutions with OH/(Al + Fe) ≤0.5. The band observed at 220 nm can be assigned to the $t_1 \rightarrow t_2$ and

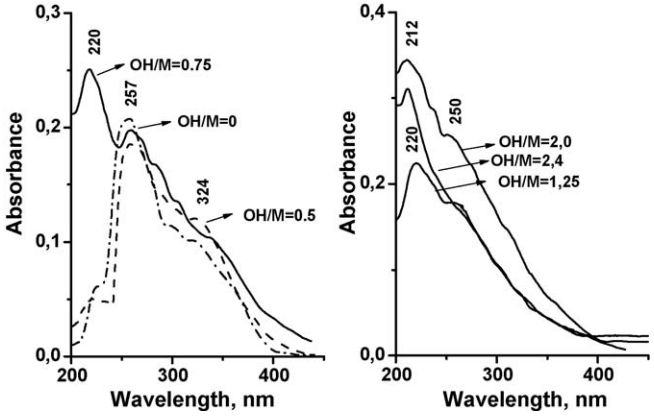

Fig. 3. UV–vis spectra of Fe,Al-solutions ($AlCl_3$ 0.016 M, Al/Fe = 10/1) at 25 °C.

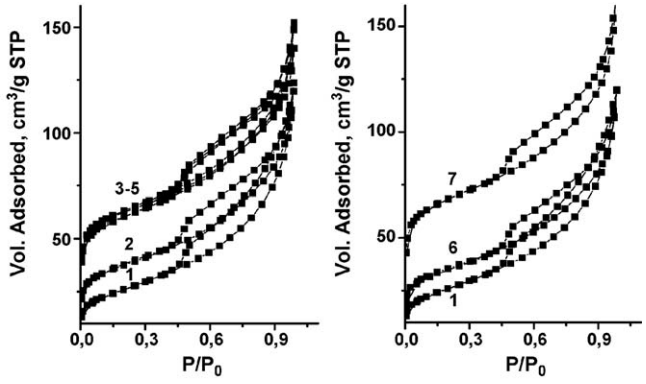

Fig. 4. N_2 adsorption/desorption isotherms of Na-clay (1), Fe,Al-PILC(I)-1 (2), Fe,Al-PILC(I)-7 (3), Fe,Al-PILC(I)-12 (4), Fe,Al-PILC(I)-21 (5), Fe,Al-PILC(II)-1 (6) and Fe,Al-PILC(II)-21 (7).

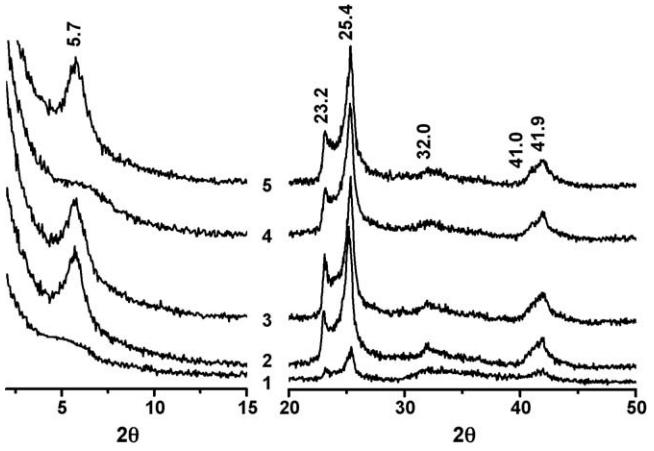

Fig. 5. X-ray diffraction patterns of Fe,Al-PILC(I)-1 (1), Fe,Al-PILC(I)-7 (2), Fe,Al-PILC(I)-21 (3), Fe,Al-PILC(II)-1 (4) and Fe,Al-PILC(II)-21 (5).

$t_1 \rightarrow$ e transitions involving Fe^{3+} in the [FeO_4] tetrahedral group. The bands at 257 and 324 nm can be attributed to a low-energy charge transfer between the oxygen ligands and the central Fe^3ion in tetrahedral and/or octahedral coordination [21,32,33]. The disappearance of bands at 257 and 324 nm and blue shift of band at 220 nm with increasing OH/(Al + Fe) ratio indicate the incorporation of Fe in Al_{13} structure.

3.2. Effect of synthesis parameters on structural and textural properties of Fe,Al-PILCs

As Table 1 suggests, the OH/(Fe + Al) ratio of pillaring solution in a region of 2.0–2.4 slightly influences on the texture characteristics of Fe,Al-PILCs. The average pore diameter decreases after intercalation of Na-clay by $FeAl_{12}$-complex. Nitrogen adsorption/desorption isotherms of Fe,Al-PILCs are shown in Fig. 4. The shape of isotherm for Na-clay is characteristic of mesoporous structures, while the shape of isotherms point out the presence of micropores in Fe,Al-PILCs [34]. Note that textural properties of Na-clay is close to that of Fe,Al-PILC(I)-1 and Fe,Al-PILC(II)-1. Fe,Al-PILC samples possess higher values of surface area and higher micropore content after intercalation of Na-clay with Fe,Al-solution aged for >7 days. The micropore volume (V_μ) is 0.046–0.054 cm^3/g that is 19–23% of the total pore-volume ($\sum V_{pore}$) of Fe,Al-PILC. This phenomenon is likely the result of dimerization of mixed Keggin cation. A similar effect was observed in the case of intercalation of montmorillonite with Al_{13}-solution [13].

Fig. 5 shows XRD patterns for Fe,Al-PILCs synthesized at 2.0 and 2.4 OH/(Fe + Al) ratio and for various aging time of Fe,Al-solution. Both parameters greatly affect the XRD patterns. A weak and broad diffraction line centered near 17.2 Å was observed in XRD patterns of Fe,Al-PILC(II)-1 and Fe,Al-PILC(I)-1. Basal reflections ($d_{0\,0\,1}$) was visualized in XRD patterns of Fe,Al-PILC after pillaring Na-clay with Fe,Al-solution aged for >7 days. The 2θ angle of the $d_{0\,0\,1}$ basal reflection was 5.7° that corresponded to the layer distance 17.8 Å. It point out the stabilization of oxide pillars due to the introduction of bulky cation into the interlayer spaces of clay that prevents its silicate layers from closing on heating.

The IR spectra of Na-clay and Fe,Al-PILC(I) samples are presented in Fig. 6. Bands at 1090 and 1047 cm^{-1} assigned to stretching vibrations of silica–oxygen tetrahedrons ν_{as}(Si–O–Si) and band at 471 cm^{-1} assigned to the bending δ(Si–O) and stretching ν(M–O) vibrations [35,36] were observed in IR spectra of Na-clay. These bands appreciably shifted in IR-spectra of Fe,Al-PILC(I) samples. It can be seen from Fig. 6, intensities of the band at 918 cm^{-1} (ν_s(O–Si–O)), bands at 624 and 527 cm^{-1} (δ(Si–O) and ν(M–O) [37]) were slightly lower for Fe,Al-PILC(I) with the 1, 7 and 21 days aged Fe,Al-solution than that for Na-clay. The shift of bands at 1090, 1047 and 471 cm^{-1} can be indirect evidence of the incorporation of Fe^{3+} into Al_{13}-polycation, because the substitution of ions Al^{3+} by Fe^{3+} should be accompanied by a general shift to high wavenumber [35]. Bands ν_{as}(Si–O–Si), δ(Si–O) and ν(M–O) are

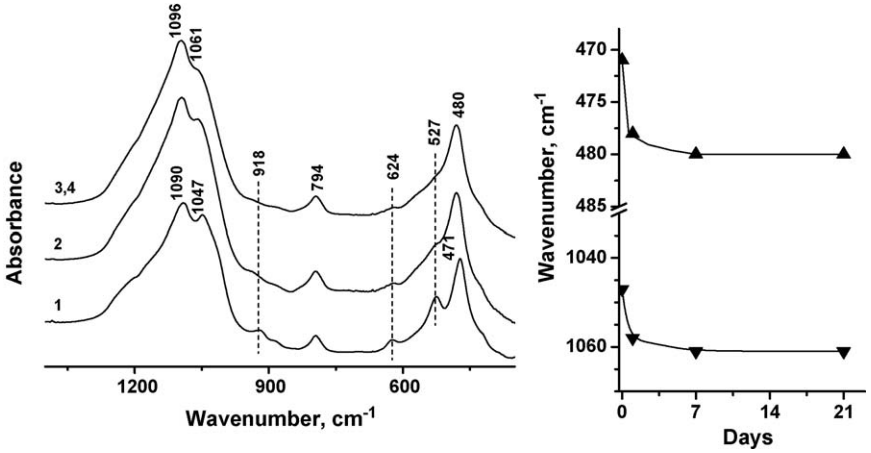

Fig. 6. IR spectra of Na-clay (1), Fe,Al-PILC(I)-1 (2), Fe,Al-PILC(I)-7 (3) and Fe,Al-PILC(I)-21 (4); and shift of bands in IR spectra.

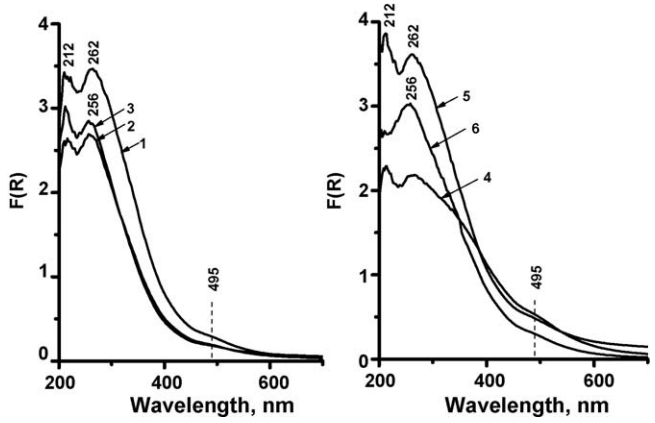

Fig. 7. DR-UV-Vis spectra of samples calcinated at 500 °C: Fe,Al-PILC(I)-1 (1), Fe,Al-PILC(I)-7 (2), Fe,Al-PILC(I)-21 (3), Fe,Al-PILC(II)-1 (4), Fe,Al-PILC(II)-21 (5) and Fe,Al-PILC(II)-21 calcinated at 400 °C (6).

the most sensitive to these substitutions. These bands shifted to high wavenumber rapidly with increasing the aging time of pillaring solution (Fig. 6). We can believe that the more shift of these bands, the higher extent of Fe^{3+} ions incorporation into Al-containing framework of polycation. The high extent of this replacement reduces to the low content of Fe_yO_x oligomeric species. DR-UV-vis data are evidence in favour of this assertion.

DR-UV-vis spectroscopy traditionally allows control the nature and coordination of iron species in iron-containing materials [33,38]. Fig. 7 shows DR-UV-vis spectra of Fe,Al-PILC synthesized at 2.0 and 2.4 OH/(Fe + Al) ratio with various aging time of pillaring solution. Two bands at 212 and 260 nm ascribed to iron species in tetrahedral and/or octahedral coordination [32,39] are observed in spectra of all Fe,Al-PILCs. The spectrum of Fe,Al-PILC(I)-1 shows band centered at ~495 nm, indicating that aggregated iron oxide clusters are formed. The intensity of this band decreases with increasing aging time of pillaring solution. Remarkable, that the intensity of bands at >260 nm was higher in spectra of Fe,Al-PILC(II)-1 and Fe,Al-PILC(II)-21 than that in spectra of Fe,Al-PILC(I)-1 and Fe,Al-PILC(I)-21. Therefore, we can postulate that Fe,Al-PILC(II) samples possess the larger quantities of extra framework iron oligomer and/or aggregated iron oxide clusters than Fe,Al-PILC(I) samples. These results clearly show that the state of iron atoms depends on OH/(Fe^{3+} + Al^{3+}) ratio [28]. Under these data it is reasonable to assume that the more this ratio, the lower agglomeration and formation of oligomeric iron species.

The nature of acid sites of Fe,Al-PILC(I)-21 was studied by IR spectroscopy. Fig. 8A shows FTIR spectrum of Fe,Al-PILC(I)-21 in the OH-stretching region. Generally, narrow bands at 3745 and 3720 cm^{-1} and broad bands in the range of 3650–3400 cm^{-1}, such as 3660 and 3358 cm^{-1}, are observed in IR spectrum of sample pre-heated at 300 °C in air. The bands at 3745 and 3720 cm^{-1} can are attributed to the stretching vibration of isolated Si–OH groups and the isolated Si–OH or Al–OH groups which slightly interact with walls of layered aluminosilicate. In addition to these isolated OH-groups, weaker broad bands in the range of 3650–3400 cm^{-1} disclose the presence of hydrogen bonded OH-groups. According to Ref. [40] band at 3660 cm^{-1} is due to structural Si(OH)Fe groups. A similar band has been observed for ferrisilicates with MFI and β structures [41,42] and Fe-alumosilicate mordenite [43]. IR spectroscopy of CO adsorbed as probe molecules was used for analysis of active sites on Fe,Al-PILC(I)-21. The spectral behavior for the CO adsorption on Fe,Al-PILC(I)-21 in the OH-stretching region is shown in Fig. 8B. One can see after CO adsorption at 80 K the band at 3745 cm^{-1} is converted into four broader bands at 3655, 3610, 3548 and 3480 cm^{-1} which can suggest the presence of several types of acid sites. Note that the red-shift of the band at 3745 cm^{-1} for pure SiO_2 (Δ_{OH} −79 cm^{-1}) is slightly lower than that for this sample (Δ_{OH} = −90, cm^{-1}). According to Refs. [44–46] bands at 3610, 3548 and 3480 cm^{-1} and can be certainty ascribed to bridging Si(OH)Al groups. Unfortunately, the band of Si(OH)Fe group can not be distinguished due to the overlapping with band of Si(OH)Al group. In carbonyl stretching region of Fe,Al-PILC(I)-21 three types of bands can be observed after spectral deconvolution (Fig. 8C). The bands at 2136 cm^{-1} (high pressure) and 2157 cm^{-1} (high pressure) were assigned to physically adsorbed CO and the CO which interacted with iron species [40,45,46], respectively. Note that the band of complex of CO with Si–OH groups can not be distinguished due to it overlapping with the band at 2157 cm^{-1}. The band at 2163 cm^{-1} (low pressure) can be attributed to the interaction of CO with Al sites [47]. Zecchina et al. [47] assigned this band to $(Al^{3+})_{oct}$–CO species. Note that a band at about 2200 cm^{-1}, which is attributed to the interaction of CO with $(Al^{3+})_{tetr}$, is absent in spectrum of Fe,Al-PILC(I)-21.

3.3. Effect of synthesis parameters on catalytic properties of Fe,Al-PILCs

3.3.1. Phenol oxidation

The experimental results on the wet phenol oxidation with H_2O_2 in the presence of Fe,Al-PILCs are summarized in Table 2. Of special note is the high activity of Fe,Al-PILCs at pH 6.0–6.2 which can be caused by the surface acidity. The mechanism of H_2O_2 decomposition is well-known and can be described by the following equations:

$$\equiv Fe^{3+} + H_2O_2 \rightarrow \equiv Fe^{2+} + HO_2^{\bullet}/O_2^{-} + H^{+} \quad (1)$$

$$\equiv Fe^{II} + H_2O_2 \rightarrow \equiv Fe^{III} + HO^{\bullet} + OH^{-} \quad (2)$$

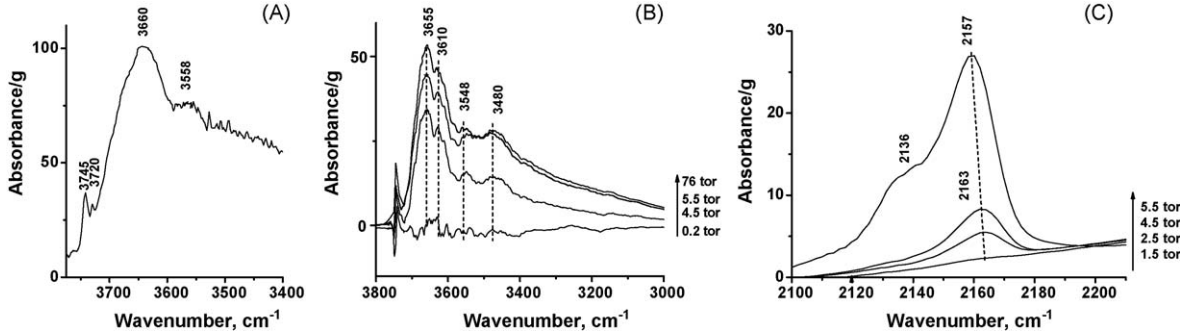

Fig. 8. (A) FTIR spectrum at 80 K of Fe,Al-PILC(I)-21 in the OH-stretching region before interaction with CO; (B) FTIR difference spectra of adsorbed CO on Fe,Al-PILC(I)-21 at 80 K (OH-stretching region). The spectrum of Fe,Al-PILC(I)-21 before interaction with adsorbate molecules (A was used for background subtraction); (C) FTIR difference spectra of adsorbed CO on the Fe,Al-PILC(I)-21 at 80 K (carbonyl stretching region).

Table 2
PhOH oxidation with H_2O_2 in the presence Fe,Al-PILCs (PhOH 1 mM, H_2O_2 14 mM, Fe,Al-PILC 1 g L^{-1}, pH 6.2, 50 °C).

No.	Catalyst[a]	Catalytic activity		Fe content		α_{PhOH}[f] (μmol m^{-2})
		Time[b] (min)	TOC removal[c] (%)	A^0_{Fe}[d] (mg g^{-1})	Δ_{Fe} (wt.%[e])	
1	Na-clay	420	0	8 ± 2	–	–
2	Fe,Al-PILC(I)-1	100	8	15 ± 1	6 ± 1	0.03
3	Fe,Al-PILC(I)-7	95	30	17 ± 1	<0.01	0.07
4	Fe,Al-PILC(I)-12	90	39	17 ± 2	<0.01	–
5	Fe,Al-PILC(I)-21	90 (90, 90)[g]	40	17 ± 1	<0.01	0.07
6	Fe,Al-PILC(II)-1	155	11	16 ± 1	14 ± 2	0.03
7	Fe,Al-PILC(II)-21	90	37	16 ± 1	<0.01	0.05
8	Fe,Al-PILC(II)-21[h]	180(180)[g]	23	15 ± 2	<0.01	–
9	Fe,Al-PILC(II)-21[h,i]	420	1	16 ± 1	12 ± 1	–

[a] Samples were calcinated at 500 °C for 2 h.
[b] Time of 100% conversion of PhOH.
[c] TOC removal after 3 h.
[d] Iron content in sample.
[e] The amount of iron leached from sample to solution (based on the initial iron content in the sample).
[f] PhOH adsorption on Fe,Al-PILC (100 mg) from aqueous solution (1 mM PhOH, 20 ml) after 24 h at 50 °C.
[g] Numbers in parentheses correspond to the second and third catalytic runs.
[h] Samples were calcinated at 400 °C 2 h.
[i] Sample was synthesized from Fe,Al-solution at Al/Fe 7/6.

According to Ref. [48] the presence of Brönsted sites in Fe,Al-PILCs are necessary to enhance the rate of Fe^{3+} reduction to Fe^{2+} and rate of phenol oxidation. Our physicochemical and catalytic data are in agreement with this assertion. The higher catalytic activity of Fe,Al-PILCs than that of Na-clay is indirect evidence that surface acidity has a dramatic impact on the reaction rate (Table 2).

As can be seen from the experimental evidence (Table 2), catalytic activity of Fe,Al-PILCs can be adjusted by iron content and calcination temperature of Fe,Al-PILCs. Since the increase in iron content leads to enlargement formation of oligomeric iron species in Fe,Al-PILC, this ensured that leaching of iron ions from Fe,Al-PILC(II) sample, which was prepared from Fe,Al-solution at Al/Fe 7/6, increases and catalytic activity of this sample decreases (Table 2, runs 8–9). The decrease of reaction rate may be good evidence that the iron oxide clusters are not active in PhOH oxidation and accelerate only H_2O_2 degradation, whereas isolated iron atoms most likely facilitate the PhOH oxidation [49]. The catalytic activity of Fe,Al-PILC(II)-21 calcinated at 400 °C was lower than that of one calcinated at 500 °C (Table 2, runs 7–8). This phenomenon also can be explained by the different state of the iron species in the Fe,Al-PILCs. One can see from DR-UV-vis spectra of these samples (Fig. 7), the great amount of extra framework iron oligomer and aggregated iron oxide clusters form after calcinated Fe,Al-PILC(II)-21 at 400 °C.

It is reasonable to suppose that calcination at 500 °C favours the high disordered structure of $FeAl_{12}^{7+}$ cation, which located into interlayer space of clay.

The aging time of pillaring solution is of importance in the providing of high activity of Fe,Al-PILCs (Table 2). Thus, the time of full phenol conversion decreases with increasing aging time of Fe,Al-solution until it reaches 12 days and then it tends to be invariable (Table 2). It is of interest that catalytic activities of Fe,Al-PILC(I)-21 and Fe,Al-PILC(II)-21 were closely, whereas activity of Fe,Al-PILC(I)-1 was higher than that of Fe,Al-PILC(II)-1. This fact can be related to the iron leaching, because the leaching of iron ions from Fe,Al-PILC(I)-1 and Fe,Al-PILC(II)-1 into solution was 6 and 14%, respectively. However the leaching of iron species was negligible for Fe,Al_2-PILCs with >7 days aged Fe,Al-solution, that can be explained by the larger content of isolated iron atoms in these samples. Note that phenol adsorption on the surface of Fe,Al-PILCs is also dictated by the aging time of Fe,Al-solution (Table 2). The adsorption values based on specific surface area of Fe,Al-PILC (α_{PhOH}) rises with increasing this parameter due to the change of content of OH-groups and isolated iron atoms which are the sites for PhOH adsorption (Table 2).

3.3.2. ACDB oxidation

The Fe,Al-PILCs samples were also tested in monoazo dye acid chrome dark-blue (ACDB) oxidation with H_2O_2 (Tables 3 and 4). It is noteworthy that kinetics of ACDB oxidation was detected by UV–vis spectroscopy at 540 nm attributed to the n–π* transition of –N=N– group (Fig. 9). The change of intensity band at 540 nm during the reaction course is presented in Fig. 9. The disappearance of this characteristic band may suggest that ACDB oxidation takes place by vanishing of azo-bond:

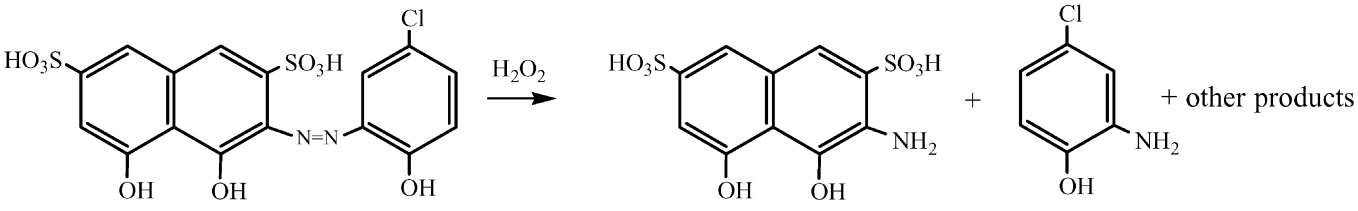

The data of the catalytic tests of Fe,Al-PILC(I)-21 indicate that this reaction strongly depends on catalyst amount, H_2O_2/ACDB ratio, pH of the reaction mixture and temperature (Figs. 10 and 11). Thus, the reaction rate increases with increasing reaction temperature and H_2O_2/ACDB ratio due to the increase of hydroxyl radical concentration (Fig. 11, Table 4, runs 2–3 and 2–4). Moreover, the increase in temperature leads to decrease in induction period caused by adsorption of ACDB on the surface

Table 3
ACDB oxidation with H_2O_2 in the presence of Fe,Al-PILCs (0.1 mM ACDB, 6 mM H_2O_2, Fe,Al-PILC 2 g L^{-1}, pH 5.8, 40 °C).

No.	Catalyst[a]	Time[b] (min)	Δ_{Fe} (wt.%)[c]	α_{ACDB} [d] (μmol m^{-2})
1	Fe,Al-PILC(I)-1	320	6 ± 0.5	0.03
2	Fe,Al-PILC(I)-7	310	<0.3	0.01
3	Fe,Al-PILC(I)-12	300	<0.3	0.01
4	Fe,Al-PILC(I)-21	300	<0.3	0.01
5	Fe,Al-PILC(II)-1	340	5 ± 0.5	0.03
6	Fe,Al-PILC(II)-21	320	<0.3	0.01

[a] Samples were calcinated at 500 °C for 2 h.
[b] Time of 100% conversion of ACDB.
[c] The amount of iron leached from sample to solution (based on the initial iron content in the sample).
[d] ACDB adsorption on Fe,Al-PILC (100 mg) from aqueous solution (0.05 mM ACDB, 5 ml) after 24 h at 25 °C.

Table 4
ACDB oxidation with H_2O_2 in the presence of Fe,Al-PILC(I) −21[a].

Run	Catalyst (g L^{-1})	Time (min)[b]	Δ_{Fe} (wt.%)[c]
1	0.75	205	2 ± 0.5
2		230	1 ± 0.5
3[d]	1.00	70	3 ± 0.5
4[e]		180	1 ± 0.5
5[f]	1.50	70	6 ± 0.5
6		205	2 ± 0.5

[a] Reaction condition: 0.1 mM ACDB, 6 mM H_2O_2, pH 5.8, 50 °C.
[b] Time of 100% conversion of ACDB.
[c] The amount of iron leached from sample to solution (based on the initial iron content in the sample).
[d] 75 °C.
[e] H_2O_2/ACDB 12/1 mol mol^{-1}.
[f] pH 3.1.

of catalyst and radical generation from H_2O_2 (Fig. 11). The maximum catalytic activity was observed at pH 3.0–4.1 of ACDB solution (Fig. 10B) that is typical for all Fenton like systems. However, the acidity affects the leaching of iron ions from Fe,Al-PILC(I)-21 into solution (Table 4, runs 2 and 5).

The aging time of pillaring solution too has a marked effect on catalytic properties of Fe,Al-PILCs (Table 3). The activity of Fe,Al-PILC(I) is higher than that of Fe,Al-PILC(II) with the 1 and 21 days aged Fe,Al-solution due to the leaching of iron ions from Fe,Al-PILCs. The increase in aging time reduced to decrease in iron leaching and time of full ACDB conversion. Note that the

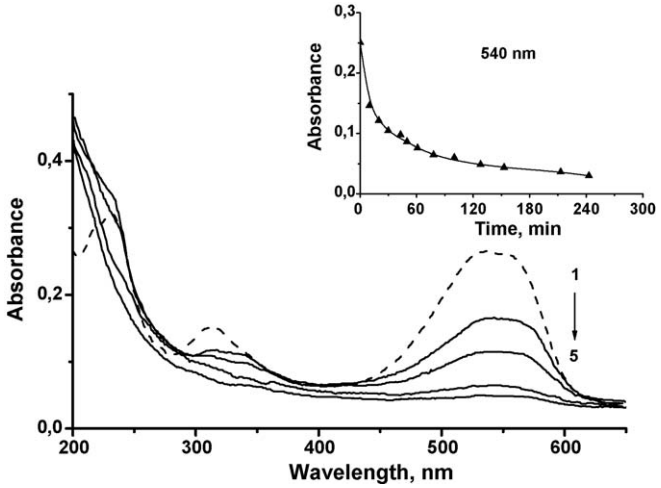

Fig. 9. UV–vis spectra of ACDB solution in the course of catalytic reaction in the presence of Fe,Al-PILC(I)-21 after 0, 30, 100, 210 and 240 min. Reaction condition: 0.1 mM ACDB, 6 mM H_2O_2, Fe,Al-PILC 2 g L^{-1}, pH 5.8 and 50 °C.

adsorption values based on specific surface area of Fe,Al-PILC (α_{ACDB}) decrease with increasing this parameter (Table 3), as differentiated from α_{PhOH} (Table 2). This difference in adsorption properties was a direct consequence of the size and configuration of PhOH and ACDB molecules. The ACDB adsorption on Fe,Al-PILCs might be depictured as coordination between iron ion and OH– and N=N-groups of ACDB:

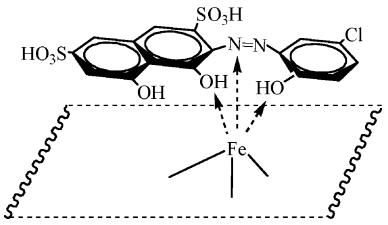

The effect of nature and content of OH-groups on the surface of samples is likely negligible for ACDB adsorption, whereas these parameters are crucial for PhOH adsorption. The more content of isolated iron species, the more content of isolated OH-groups, and so the more α_{PhOH} (Table 2). It is believed that the slightly larger adsorption value of ACDB on Fe,Al-PILC(I-II)-1 than that on Fe,Al-

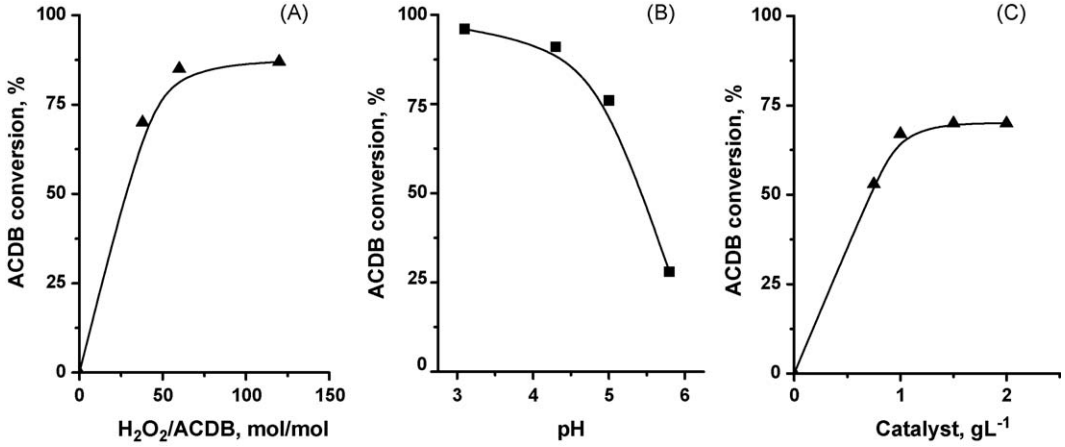

Fig. 10. The effect of H_2O_2/ACDB ratio, catalyst loading and initial pH acidity on ACDB removal in the presence of Fe,Al-PILC(I)-21. (A) 0.1 mM ACDB, Fe,Al-PILC(I)-21 1 g L^{-1}, pH 5.9, 50 °C, 100 min; (B) 0.1 mM ACDB, 6 mM H_2O_2, Fe,Al-PILC(I)-21 1 g L^{-1}, 50 °C, 15 min; (C) 0.1 mM ACDB, 6 mM H_2O_2, pH 5.9, 50 °C, 50 min.

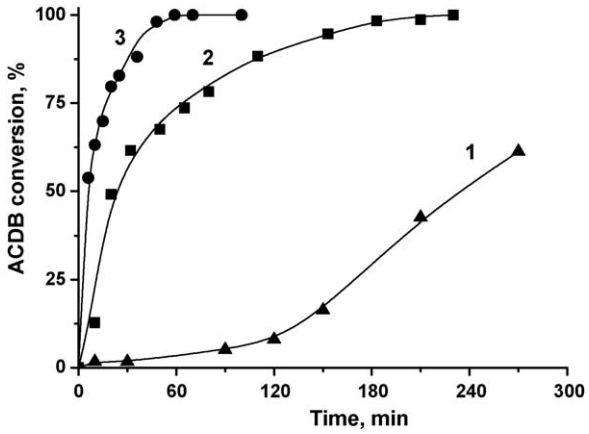

Fig. 11. The ACDB consumption in the presence of 1.0 g L^{-1} Fe,Al-PILC(I)-21 at 25 °C (1), 50 °C (2) and 75 °C (3) (0.1 mM ACDB, 6 mM H_2O_2, Fe,Al-PILC(I)-21 1 g L^{-1}, pH 5.9).

PILC(I-II)-21 results from difference in textural properties. The low microporosity of Fe,Al-PILC(I-II)-1 promotes the high accessibility of Fe sites for ACDB adsorption. However the high accessibility of Fe affects adversely on the iron leaching induced by the reagents and/or products (Table 3). Thus, the iron leaching was high in ACDB oxidation and reached 0.3% from total iron content in Fe,Al-PILC(I)-21. However, no loss of the catalytic activity was observed after at least 2 catalytic cycles of PhOH oxidation in the presence of this sample due the stability to leaching with respect to PhOH (Table 2).

4. Conclusion

It has been shown that textural properties of Fe,Al-containing pillared clay can be controlled by OH/(Fe + Al) ratio, the calcination temperature and aging time of pillaring solution. The prolonged aging time of the Fe,Al-solution (Al/Fe = 10/1) favours the increase in the total surface area, total pore-volume and micropore volume. The higher value of surface area and higher content of micropore were observed in Fe,Al-PILC samples after intercalation of Na-PILC with Fe,Al-solution aged for >7 days. The influence of OH/(Fe + Al) ratio on textural properties was negligible in the region of 2.0–2.4. At the same time this ratio was important for the formation oligomeric iron oxide clusters. Isolated iron species predominate when OH/(Fe + Al) ratio is 2.4. The Al/Fe ratio and calcination temperature affect the state of the iron species in the Fe,Al-PILCs. The increase in Al/Fe ratio and calcination temperature from 400 to 500 °C reduces to the increase in the formation of isolated iron species. Fe,Al-PILCs were tested as catalysts for wet phenol and monoazo dye acid chrome dark-blue with H_2O_2. It was shown that the increase in aging time of Fe,Al-pillaring solution reduced to decrease in iron leaching and time of full reagents conversion. Isolated iron species predominate in Fe,Al-PILC under OH/(Fe + Al) ratio 2.4 and Fe,Al-solution aged for >1 day. This sample was stable to leaching of iron species and highly active in phenol and ACDB peroxide oxidation.

Acknowledgements

This work was supported by Russian Foundation for Basic Research under Grant 07-90100-a, 06-08-01064-a and 08-08-00729-a. The authors would like to thank Dr. A.V. Golovin for valuable discussion and comments for ^{27}Al NMR data.

References

[1] R. Szostak, C. Ingram, Stud. Surf. Sci. Catal. 94 (1995) 13.
[2] H. Debellefontaine, M. Chakchouk, J.N. Foussard, D. Tissot, P. Striolo, Environ. Pollut. 92 (2) (1996) 155.
[3] C. Walling, Acc. Chem. Res. 31 (4) (1998) 155.
[4] G. Centi, S. Perathoner, T. Torre, M.G. Verduna, Catal. Today 55 (2000) 61.
[5] N. Crowther, F. Larachi, Appl. Catal. A: Environ. 46 (2003) 293.
[6] J. Carriazo, E. Guélou, J. Barrault, J.M. Tatibouët, R. Molina, S. Moreno, Catal. Today 107/108 (2005) 126.
[7] M.N. Timofeeva, S.C. Khankhasaeva, S.V. Badmaeva, A.L. Chuvilin, E.B. Burgina, A.B. Ayupov, V.N. Panchenko, A.V. Kulikova, Appl. Catal. B: Environ. 59 (2005) 243.
[8] A. Gil, S.A. Korili, M.A. Vicente, Catal. Rev. Sci. Eng. 50 (2008) 153.
[9] J.T. Kloprogge, L.V. Duong, R.L. Frost, Environ. Geol. 47 (2005) 967.
[10] J. Barrault, C. Bouchoule, J.-M. Tatibouët, M. Abdellaoui, A. Majesté, I. Louloudi, N. Papayannakos, N.H. Gangas, Stud. Surf. Sci. Catal. 130 (2000) 749.
[11] N.D. Hutson, M.J. Hoekstra, R.T. Yang, Micropor. Mesopor. Mater. 28 (1999) 447.
[12] A. Gil, A. Diaz, M. Montes, D.R. Acosta, J. Mater. Sci. 29 (1994) 4927.
[13] Y.S. Shin, S.G. Oh, B.H. Ha, Korean J. Chem. Eng. 20 (1) (2003) 77.
[14] W.O. Parker Jr., I. Kiricsi, Appl. Catal. A: Gen. 121 (1995) L7.
[15] I. Palinko, A. Molnar, J.B. Nage, J.C. Bertrand, K. Lazar, J. Valyon, I. Kiricsi, J. Chem. Soc., Faraday Trans. 3 (1997) 1591.
[16] D. Zhao, G. Wang, Y. Yang, X. Guo, Q. Wang, J. Ren, Clays Clay Minerals 41 (1993) 317.
[17] A. Gil, L.M. Gandia, M.A. Vicente, Catal. Rev.-Sci. Eng. 42 (1/2) (2000) 145.
[18] W.Y. Lee, R.H. Raythatha, D.B.J. Tatarchuk, J. Catal. 115 (1989) 159.
[19] L.K. Lepin, A.Ya. Vaivade, Zh. Phys. Chem. 27 (1953) 217.
[20] J.Y. Bottero, J.M. Flessinger, J.E. Polrter, J. Phys. Chem. 84 (1980) 2933.
[21] J. Duan, J. Gregory, Adv. Colloid Interf. Sci. 100–102 (2003) 475.
[22] L. Storaro, M. Lenarda, R. Ganzerla, A. Rinaldi, Micropor. Mater. 6 (1996) 55.
[23] J.M. Akitt, N.N. Greenwood, B.L. Khandelwal, G.D. Laster, J. Chem. Soc., Dalton Trans. 5 (1972) 604.
[24] M.M. Clark, R.M. Srivastave, Environ. Sci. Technol. 27 (1993) 2181.
[25] Z. Chen, Z. Luan, J. Fan, Z. Zhang, X. Peng, B. Fan, Colloids Surf. A: Physicochem. Eng. Aspects 292 (2007) 110–118.
[26] R.B. Martin, J. Inorg. Biochem. 44 (1991) 141.
[27] S.M. Bradley, R.A. Kydd, J. Chem. Soc., Faraday Trans. 5 (1993) 2407.
[28] A. Schutz, W.E.E. Stone, G. Pongelet, J.J. Fripiat, Clay Clay Minerals 35 (1987) 251.
[29] T.J. Pinnavaia, M.S. Tzou, S.D.L. Landau, R.H. Raythatha, J. Mol. Catal. 27 (1984) 195.
[30] J.W. Akitt, N.N. Greenwood, B.L. Kladelwal, G.D. Lester, J. Chem. Soc., Dalton Trans. (1972) 604.
[31] C. Feng, H. Tang, D. Wang, Colloids Surf. A: Physicochem. Eng. Aspects 305 (2007) 76.
[32] D.M. Sherman, Phys. Chem. Minerals 12 (1985) 161.
[33] S. Bordiga, R. Buzzoni, F. Geobaldo, C. Lamberti, E. Giamello, A. Zecchina, G. Leofanti, G. Petrini, G. Tozzola, G. Vlaic, J. Catal. 158 (1996) 486.
[34] R. Mokaya, W. Jones, J. Porous Mater. 1 (1995) 97.
[35] P. Wu, T. Komatsu, T. Yashima, Micropor. Mesopor. Mater. 20 (1998) 139.
[36] G.J. Kim, W.S. Ahn, Zeolites 11 (1991) 745.
[37] V.C. Farmer, The Infrared Spectra of Minerals, Mineral Soc., London, 1974.
[38] B.N. Figgis, Introduction to Ligan Fields, Wiley, New York, 1966.
[39] Y. Li, Zh. Feng, Y. Lian, K. Sun, L. Zhang, G. Jia, Q. Yang, C. Li, Micropor. Mesopor. Mater. 84 (2005) 41.
[40] K.I. Hadjiivanov, G.N. Vayssilov, Adv. Catal. 47 (2002) 307.
[41] C.T.W. Chu, C.D. Chang, J. Phys. Chem. 89 (1985) 1569.
[42] R. Kumar, A. Thangaraj, R.N. Bhat, P. Ratnasamy, Zeolites 10 (2) (1990) 85.
[43] P. Wu, T. Komatsu, T. Yashima, Micropor. Mater. 20 (1998) 139.
[44] J. Cejka, B. Wichterlova, Catal. Rev. 44 (3) (2002) 375.
[45] H. Knozinger, S. Huber, J. Chem. Soc., Faraday Trans. 94 (15) (1998) 2047.
[46] M. Sigl, S. Ernst, J. Weitkamp, H. Knozinger, Catal. Lett. 45 (1997) 27.
[47] A. Zecchina, E. Platero, A. Otero, J. Catal. 107 (1987) 244.
[48] S. Letaief, B. Casal, P. Aranda, M.A. Martin-Luengo, E. Ruiz-Hitzky, Appl. Clay Sci. 22 (2003) 263.
[49] M.N. Timofeeva, M.S. Mel'gunov, O.A. Kholdeeva, M.E. Malyshev, A.N. Shmakov, V.B. Fenelonov, Appl. Catal. B: Environ. 75 (2007) 290.